

Elasticity of DNA and the effect of Dendrimer Binding

Santosh Mogurampelly,* Bidisha Nandy, and Prabal K. Maiti

Centre for Condensed Matter Theory, Department of Physics,

Indian Institute of Science, Bangalore - India 560012.

Roland R. Netz

Fachbereich Physik, Freie Universität Berlin, 14195 Berlin, Germany.

Abstract

Negatively charged DNA can be compacted by positively charged dendrimers and the degree of compaction is a delicate balance between the strength of the electrostatic interaction and the elasticity of DNA. We report various elastic properties of short double stranded DNA (dsDNA) and the effect of dendrimer binding using fully atomistic molecular dynamics and numerical simulations. In equilibrium at room temperature, the contour length distribution $P(L)$ and end-to-end distance distribution $P(R)$ are nearly Gaussian, the former gives an estimate of the stretch modulus γ_1 of dsDNA in quantitative agreement with the literature value. The bend angle distribution $P(\theta)$ of the dsDNA also has a Gaussian form and allows to extract a persistence length, L_p of 43 nm. When the dsDNA is compacted by positively charged dendrimer, the stretch modulus stays invariant but the effective bending rigidity estimated from the end-to-end distance distribution decreases dramatically due to backbone charge neutralization of dsDNA by dendrimer. We support our observations with numerical solutions of the worm-like-chain (WLC) model as well as using non-equilibrium dsDNA stretching simulations. These results are helpful in understanding the dsDNA elasticity at short length scales as well as how the elasticity is modulated when dsDNA binds to a charged object such as a dendrimer or protein.

*Corresponding author; Electronic address: santosh@physics.iisc.ernet.in; santoshcup6@gmail.com

I. INTRODUCTION

Many fundamental biological processes of life such as DNA replication, translation and transcription involve interaction of DNA with proteins where the elasticity of DNA is crucial as a short segment of DNA is tightly wound around proteins. The length scales involved in such biological processes are less than the persistence length (50 nm) of dsDNA and are of interest to study. The advancement of micromanipulation techniques in the last decades allows to perform manipulation experiments with single molecule DNA to understand its mechanical properties. Elastic properties of short DNA of few 10's of base-pairs play a significant role in many cellular processes [1–3]. Extensive experimental work has been done on DNA elasticity in the decade [4–8], but most studies involve long DNA of more than few hundreds of base-pairs in length. Many cellular processes involve unzipping of local DNA base-pairs when proteins bind to DNA with specific interactions [9, 10]. Poly amido amine (PAMAM) dendrimers are hyperbranched polymers and can be considered as model proteins with many protein-like structural similarities [11–13]. PAMAM dendrimers are positively charged at neutral and low pH [14] and can bind negatively charged DNA. Earlier we have studied the interaction of DNA with a dendrimer [15, 16] at varying pH conditions and showed that the binding energy of the DNA-dendrimer complex increases with the size of the dendrimer [16]. In this paper we try to understand how the elasticity of DNA is altered while complexed with a dendrimer, which can be viewed as a model protein. The length scale of the binding area at the DNA binding site covered by typical proteins spans few base-pairs, which is similar to the size of dendrimers.

The end-to-end distance (R) distributions ($P(R)$) of semi-flexible polymers in the context of their elasticity have been studied in the past decade extensively [17–25]. Recently both experiments and simulations have focused on the short length scales to study the elasticity of short dsDNA [26–29]. Mazur [30–33] has studied the elastic properties of dsDNA using atomistic simulations based on the probability distributions of end-to-end distance, bending angle etc. To study the effect of dendrimer binding, recent studies [34, 35] using small angle X-ray scattering revealed that dsDNA has different bending modes depending on the dendrimer charge density. The case of a semi-flexible polymer interacting with an oppositely charged sphere was treated as a simple model case of DNA wrapping around

histones, forming nucleosome core particles (NCP). This study revealed how the wrapping propensity is influenced by the ionic strength of the solution [9, 10] and how structures very similar to chromatin appear [36]. Understanding short length scale elastic behavior of dsDNA is important since the local bending and unzipping of dsDNA can occur when it binds to proteins. The length scales over which protein binds to dsDNA in a DNA-protein complex are in the nano meter scale, which is less than the persistence length of dsDNA. However, models based on worm-like chain (WLC) largely fails to explain elastic behavior of dsDNA on such short length scales.

With the advance of single molecule experimental techniques like optical tweezers, magnetic tweezers and atomic force microscopy (AFM), it has become possible to study structural details of single DNA (both dsDNA and ssDNA) under external force at varying physiological conditions. Several experimental and theoretical groups have studied [5, 8, 37–42] structural transformations of DNA by external force pulling at one end and fixing the other end of the dsDNA. Single molecule experimental studies of DNA elasticity are explained well by worm-like-chain model [8, 43] which assumes inextensibility, isotropic bending rigidity of polymer in the thermodynamic limit ($L/L_p \rightarrow \infty$; where L_p is the persistence length) [5, 8]. WLC theory gives the average end-to-end distance of the polymer when stretched with a force that involves the initial contour length and the persistence length as fitting parameters. However, the WLC model fails to explain the force-extension behavior in the large force limit and also for short length of polymers. For example, for short DNA molecules the WLC model is inadequate to explain the elastic behavior and gives incorrect estimate of persistence length [26, 44], an intrinsic property of the polymer that is expected to be independent of the contour length. In a recent study [27], it has been shown that shorter DNA is softer than measured by single-molecule experiments. It was also shown that the variance in end-to-end distance has a quadratic dependence on the number of base-pairs rather than a linear dependence, a result of linear elastic rod model [44]. These failures of the WLC are mainly due to finite length effects, boundary conditions and rotational fluctuations at the force attachment. Some of these corrections have been incorporated into the WLC model and led to a more general model called FWLC (Finite WLC) in ref [45]. The finite WLC model is able to predict force-extension for a wide range of forces for polymers with lengths ranging from less than the persistence length to infinite chain limit

[45]. It can also include the effect of formation of a single permanent kink in the polymer. Several researchers have studied the force-extension behavior of polymers, single and double stranded DNA with improvements to the standard WLC model [26, 45–50] but a complete understanding of the elastic behavior at various length scales is not yet well established.

In this paper, we use numerical simulations to solve the WLC model and obtain the end-to-end distance distribution as done earlier [19]. Supported by the WLC numerical solution, we demonstrate that the full atomic description of dsDNA can give more insight into the elasticity at short length scales and how the elastic properties of short dsDNA change when binding to a dendrimer. From the equilibrium contour length and bending angle distributions of 38 base-pair dsDNA, we calculate the stretch modulus and bending persistence length of dsDNA. The variance of the end-to-end distance has a nearly quartic dependence on the number of base-pairs of dsDNA which has its origin in bending fluctuations. By stretching the bare dsDNA in solvent, we calculate the force-extension curves. The stretch modulus calculated from zero and finite-force methods is in good agreement with experiments.

II. METHODS

All atom molecular dynamics simulations of DNA in salt solution were carried out in equilibrium as well as in non-equilibrium. The sequence of 12 base-pair DNA used in our simulation is d(CGC GAA TTC GCG)₂, and that for 38 base-pair DNA is d(GCC GCG AGG TGT CAG GGA TTG CAG CCA GCA TCT CGT CG)₂ and was taken from our earlier works [41, 42, 51, 52]. To study the effect of dendrimer binding on the elasticity of DNA, we have used the G3 PAMAM dendrimer and 38 base-pair dsDNA complex at neutral pH as reported earlier [16]. In equilibrium, 38 base-pairs dsDNA and dendrimer bound 38 base-pairs dsDNA were simulated separately in explicit solvent. We use ff03 force field parameters of Duan *et. al.* [53] to describe the bonded and non-bonded interactions for DNA and the TIP3P model [54] for water. We have used the DREIDING force field [55] to describe the intermolecular interaction of the dendrimer. The box dimensions were chosen in order to ensure a minimum of 10 Å solvation shell around the DNA structure during

all simulations. The bare DNA system is neutralized with Na^+ counterions and dendrimer bound DNA is neutralized with Na^+ as well as Cl^- counterions to account for the negative charge on DNA and positive charge on dendrimer. Total system size for equilibrium simulations is 34783 atoms for bare DNA and 179234 atoms for dendrimer bound DNA including water and counterions. For non-equilibrium stretching of 12 base-pair DNA and 38 base-pair DNA, both strands of one end of dsDNA were pulled with an external force which increased linearly with time. The other end of the dsDNA was held fixed. During pulling, we measure the extension of the dsDNA as a function of the applied force. For the stretching simulations, we have added extra water along the pulling direction to ensure solvation of DNA even in fully stretched condition. With this, the system size of 38 base-pair bare DNA increases to 97326 atoms. The total number of atoms including water and counterions for the stretching simulation of 12 base-pair DNA is 27858. The system energy was minimized by 1000 steps of steepest descent minimization followed by 2000 steps of conjugate gradient minimization. Translational center-of-mass motions were removed after every 1000 steps. NPT-MD was used to get the correct solvent density corresponding to experimental condition. The long range electrostatic interactions were calculated with the Particle Mesh Ewald (PME) method [56]. A real space cut off of 9 Å was used both for the long range electrostatic and short range van der Waals interactions. We have used periodic boundary conditions in all three directions during the simulation. During the simulation, bond lengths involving bonds to hydrogen atoms were constrained using SHAKE algorithm [57]. For the equilibrium simulation we have simulated the bare dsDNA for 85 ns and dendrimer bound dsDNA was simulated for 70 ns. For the stretching of dsDNA, we continue the simulation until we get a fully stretched dsDNA. The time scale of the simulation at which we get fully stretched DNA depends on the rate of pulling. For 12 base-pair DNA we use a pulling rate of 10^{-5} pN/fs which requires about 40 ns and for 38 base-pair DNA stretching we use 10^{-4} pN/fs which requires 10 ns to get the DNA in the fully stretched form.

From the MD trajectories of both the bare DNA and dendrimer bound DNA simulation, we have calculated the helix axis, end-to-end distance and contour length using Curves algorithm developed by Skelnar and Lavery[58]. All of these parameters are calculated as a function of each base-pair step n . Using these parameters we have analyzed the contour length distribution $P(L)$, end-to-end distance distribution $P(R)$, bending angle distribution

$P(\theta)$, variance of end-to-end distance σ_n^2 and compared them with those obtained from WLC model. The WLC model is solved numerically to get $P(R)$ and force-extension curves for polymers of any length ranging from highly flexible ($L \gg L_p$) to highly stiff ($L \ll L_p$) polymers. Force-extension curves were also obtained from MD simulations with external force.

III. RESULTS AND DISCUSSION

A. Equilibrium properties of dsDNA

1. Contour length distribution $P(L)$

In equilibrium at room temperature, the instantaneous contour length (L) of dsDNA has thermal fluctuations around its mean contour length L_0 . The instantaneous contour length, L is defined as the sum of all n base-pair rises, $L = \sum_{i=0}^n h_i$, where h_i is i^{th} base-pair rise as shown in Figure 1(a). A small instantaneous fluctuation ($L - L_0$) in contour length around its mean value L_0 generates a restoring force F in the dsDNA that is proportional to $L - L_0$, such that $F = -\gamma_1 (L - L_0) / L_0$, where γ_1 is the stretch modulus of dsDNA. The free energy due to this restoring force can be obtained by integrating the force F with respect to contour length, $E(L) = \frac{\gamma_1}{2L_0} (L - L_0)^2$. Plugging $E(L)$ into the Boltzmann factor $e^{-\beta E(L)}$, for obtaining the probability of having a length L with energy $E(L)$ and normalizing gives

$$P(L) = \sqrt{\frac{\gamma_1 L_0}{2\pi k_B T}} e^{-\frac{\gamma_1 L_0}{2k_B T} (L/L_0 - 1)^2} \quad (1)$$

$$\implies \ln P(L) = -\frac{\gamma_1 L_0}{2k_B T} (L/L_0 - 1)^2 + C \quad (2)$$

We have analyzed equilibrium simulation trajectories for studying fluctuations in the contour length of the dsDNA. Contour length distributions $P(L)$ are shown in Figure 1(b) for bare and dendrimer bound DNA. The contour length distribution for bare and dendrimer bound DNA is very sharp with a small width. It means that DNA is stiff with small variance in contour length. By fitting $P(L)$ to a Gaussian, we obtain the stretch modulus γ_1 to be 955 pN for bare DNA and 959 pN for dendrimer bound DNA. The calculated value of the stretch modulus for bare dsDNA is in good agreement with experimental reports

[4–6] and simulations [41, 42]. We can see that the dendrimer bound DNA is significantly bent around dendrimer compared to bare DNA which is almost straight. But the bending of DNA around dendrimer does not alter the stretch modulus since the contour length is almost independent of the degree of DNA bending. We have also calculated the end-to-end distance distribution, $P(R)$ to estimate the degree of bending of DNA around dendrimer. $P(R)$ and snapshots of bare DNA and dendrimer bound DNA are shown in Figures 1(c), 1(d) and 1(e), respectively. Note that due to the bending of dsDNA, the width of the end-to-end distribution of dendrimer bound DNA is very large compared to the width of the distribution for the bare DNA.

To calculate the bending persistence length L_p as well as the bending modulus κ , we calculate the distribution of bending angle $P(\theta)$. The bending angle θ is defined as the angle between tangents $t(s)$ and $t(s')$. Similar to the contour length fluctuations, small fluctuation in θ can be approximated to be of Gaussian nature and can be written as

$$P(\theta) = \sqrt{\frac{\kappa}{2\pi|s^1 - s^n|_{av}k_B T}} e^{-\frac{\kappa}{2|s^1 - s^n|_{av}k_B T}\theta^2} \quad (3)$$

$$\implies \ln P(\theta) = -\frac{L_p}{|s^1 - s^n|_{av}}(1 - \cos \theta) + C \quad (4)$$

where $|s^1 - s^n|_{av}$ is the average contour length (L_0), $\frac{\kappa}{k_B T} = L_p$ and κ is the bending modulus of DNA. From the simulation trajectories of 38 base-pair DNA, we have analyzed $P(L)$ and $P(\theta)$ for different base-pair lengths n between 1 to 38 base-pairs as shown in Figures 2(a) and 2(b), respectively. $P(L)$ for all base-pair lengths is Gaussian (Figure 2(a)). $\ln P(\theta)$ versus $(1 - \cos \theta)$ is plotted in Figure 2(b). $\ln P(\theta)$ is linear in $(1 - \cos \theta)$ and from the fit, we obtain the persistence length, L_p to be 43 nm which is close compared to the standard experimental value of 50 nm. The bending modulus κ of bare DNA obtained from our simulation is 1.76×10^4 pN \AA^2 .

Do the stretch modulus and persistence length calculated from our atomistic MD simulation conform to the idea that DNA can be treated as an isotropic elastic rod? To probe this we note that for the isotropic elastic rod model, the stretch modulus γ_1 is related to the persistence length as follows: $L_p = \gamma_1 r^2 / 4k_B T$, where r is the radius of DNA. Using $r = 1$ nm and $L_p = 43$ nm, we estimate γ_1 for bare DNA to be 705 pN as compared to $\gamma_1 = 955$ pN from contour length distribution. Conversely, for an effective radius of $r=0.86$

nm, the isotropic elastic rod model works perfectly. For dendrimer bound DNA, we find an effective persistence length of $L_p = 6.3$ nm from our analysis of end-to-end distance distribution, and again using elastic rod formula we estimate γ_1 of dendrimer bound DNA to be 103 pN. This is very small compared to the value of 959 pN obtained from contour length distribution. This implies that dendrimer bound DNA is more flexible than bare DNA. Dendrimer is a flexible molecule with positive charges on the primary amine groups on the periphery. The branches are mobile making the positive charges moving along the negative charges. When positively charged dendrimer binds to negatively charged DNA, charge neutralization happens reducing the phosphate-phosphate repulsion in the DNA backbone and the stiffness of DNA is much reduced. This also causes DNA to bend around dendrimer. We expect similar situations to arise when proteins bind to DNA which will be the subject of future study.

2. Correlations in fluctuations of dsDNA base-pairs

Mathew-Fenn *et. al.* [27] have studied DNA flexibility at short length scales using the variance in the end-to-end distance obtained using small angle X-ray scattering techniques. They have tethered clusters of gold atoms to 3' thiol linker of DNA ends and measured the distributions of end-to-end distance for various DNA length of base-pairs ranging from 10 to 35. By fitting $P(R)$ to a Gaussian form, they observe that the variance σ_n^2 is quadratic with the number of base-pairs n in DNA. Motivated by this study, we also calculate the correlations in fluctuations of $P(R)$ for dsDNA base-pairs. Here, we ask how the room temperature fluctuations of individual base-pairs are correlated with the neighboring base-pairs in dsDNA by looking at the variance σ_n^2 in the end-to-end distance, R of dsDNA. We write,

$$\sigma_n^2 = \langle (R_n - R_{n0})^2 \rangle \quad (5)$$

where R_n is the end-to-end distance of n base-pairs and R_{n0} is its average value. We have shown σ_n^2 as a function of number of the base-pairs n in Figure 3 for bare DNA and dendrimer bound DNA, respectively. The inset shows end-to-end distance which is proportional to n . We fit the simulation data to $\sigma_n^2 = an + bn^4$, which describes the

data very well. Fitting parameters are $a = 0.02359 \text{ \AA}^2, b = 0.00000356 \text{ \AA}^2$ for bare DNA and $a = -0.07891 \text{ \AA}^2, b = 0.0000291 \text{ \AA}^2$ for dendrimer bound DNA. The quartic term is due to bending fluctuations, while the linear term accounts for the possible presence of stretching fluctuations. Our results on σ_n^2 are thus only partially consistent with Mathew-Fenn *et. al.* [27]. Here it is worth mentioning that this issue of cooperative base-pair fluctuation and its relevance in the context of quadratic dependence of the variance of the end-to-end distance has been discussed in the literature extensively in last few years [29–33]. Mazur attributed this quadratic dependence to the incomplete subtraction of the bending contribution from the end-to-end distance variance. Becker and Everaers [59] attributed this to subtle linker leverage effect and concluded that when the linker effect is subtracted from the variance data, the dependence will be linear. However, recent work by Noy and Golestanian [60] shows that indeed the quadratic dependence exists even after the bending contribution is removed. They attribute this to different modes of deformation in the DNA structure. Our results seem not to be in line with the results by Noy and Golestanian [60]. More efforts are needed for a complete understanding of this issue.

3. Worm-like chain model (WLC)

The worm-like chain (WLC) model (or Kratky-Porod model) for the force-extension relation was proposed to explain the elasticity of polymers [8, 43]. Disadvantage is that analytical results can be obtained only in the asymptotic limits. By solving WLC model with the help of numerical evaluation, we show that the model can be applied to polymers of small L_0 ($< L_p$) to a good approximation. We apply this method to study the elasticity of dsDNA. The results are then compared to the results obtained from MD simulations of 38 base-pair dsDNA whose length is about $0.25 L_p$. We also try to connect the effect of a dendrimer binding on the elasticity of dsDNA.

At room temperature, fluctuations in dsDNA are induced by thermal agitations. The worm-like chain model assumes that the polymer is a continuous chain with energy given by

$$\hat{H} = \frac{\kappa}{2} \int_0^{L_0} \left(\frac{d\hat{t}(s)}{ds} \right)^2 ds \quad (6)$$

where $\hat{t}(s)$ is the tangent vector at s on the space curve as shown in the schematic in Figure 4(a), with s changing from 0 to L_0 , contour length of the polymer and κ is the bending modulus of the polymer. The persistence length of the polymer is defined as $L_p = \frac{\kappa}{k_B T}$, where k_B is the Boltzmann constant.

The numerical solution of the WLC model is described in detail by Samuel and Sinha [19]. Here we give a brief outline of the method. Suppose that we apply a force on the WLC polymer at one end in the z -direction. The new Hamiltonian can be written as,

$$\hat{H} = \int_0^{L_0} \left[\frac{\kappa}{2} \left(\frac{d\hat{t}(s)}{ds} \right)^2 - f t_z \right] ds. \quad (7)$$

Substituting $\kappa = L_p k_B T$ and changing variable to $\tau = s/L_p$, we obtain the dimensionless Hamiltonian as,

$$\Rightarrow \frac{\hat{H}}{k_B T} = \int_0^{L_0/L_p} \left[\frac{1}{2} \left(\frac{d\hat{t}(\tau)}{d\tau} \right)^2 - \frac{L_p f}{k_B T} t_z \right] d\tau. \quad (8)$$

Now we use $\beta = L_0/L_p$ and $\tilde{f} = \frac{L_p f}{k_B T}$ to obtain the partition function as,

$$Z(\tilde{f}) = N \int D[\hat{t}(\tau)] e^{-\int_0^\beta d\tau \left[\frac{1}{2} \left(\frac{d\hat{t}}{d\tau} \right)^2 - \tilde{f} t_z \right]} \quad (9)$$

here $\beta = L_0/L_p$ is analogous to the inverse temperature. Proper choice of the basis set is crucial for the numerical evaluation of Z . In 3D, the natural choice are the spherical harmonics $|l\rangle = Y_{l,0}(\theta, \phi)$ which are angular part of the normalized eigenfunctions of $-\nabla^2/2$. To compute $Z(\tilde{f}) = \langle 0 | e^{-\frac{\nabla^2}{2} - \tilde{f} \cos \theta} | 0 \rangle$, we have used the following basis set to include force \tilde{f}

$$\langle l | \hat{H} | l' \rangle = \frac{l(l+1)}{2} \delta_{l,l'} - \frac{\tilde{f}(l+1)}{\sqrt{(2l+1)(2l+3)}} (\delta_{l+1,l'} + \delta_{l,l'+1}). \quad (10)$$

By calculating $Z(\tilde{f})$ numerically to a desired accuracy, we can calculate various properties of the system. The end-to-end distance distribution is calculated using, $P(R) = -2R \frac{dp(R)}{dR}$ [19], where $p(R)$ is the inverse Fourier transform (by working with imaginary \tilde{f}) of the partition function $Z(\tilde{f})$. The resulting expression for $P(R)$ is given by

$$P(R) = \frac{2R}{\pi} \int_0^\infty dk k Z(ik) \sin kR \quad (11)$$

where $Z(ik)$ is the partition function under the effect of an imaginary force $\tilde{f} = ik$. We also calculate the force \tilde{f} versus extension ϵ behavior and the free energy $G(\tilde{f})$, of the system as follows,

$$\epsilon = -\frac{dG(\tilde{f})}{d\tilde{f}} \quad (12)$$

and

$$G(\tilde{f}) = -\frac{1}{\beta} \ln Z(\tilde{f}) \quad (13)$$

Where the extension ϵ is the ratio of the end-to-end distance to the fixed contour length of DNA, i.e., $\epsilon = R/L_0$. These quantities can be measured experimentally giving a direct validation of the model. $P(R)$ and ϵ are plotted in Figure 4. $P(R)$ for various values of β as a function of R/L_0 is plotted in Figure 4(a). For flexible polymers, $\beta \gg 1$ and for stiff polymers, $\beta \ll 1$ while for semi-flexible polymers β has intermediate values. In Figure 4(a), $P(R)$ has a peak at low values of R/L_0 for flexible polymers where as the peak appears at large values of R/L_0 for semi-flexible or stiff polymers. This is due to the difference in the energy cost for bending. The energy cost for bending is less for flexible polymers compared to semi-flexible polymers. Flexible polymers are in coiled form since $L_0 \gg L_p$ where as semi-flexible polymers have length comparable to L_p . We plot $P(R)$ of bare DNA and dendrimer bound DNA in Figure 4(a) for comparison. Bare DNA has peak at $R/L_0 = 0.95$ and dendrimer bound DNA has peak at $R/L_0 = 0.84$ indicating the more flexible nature of DNA when bound to dendrimer. Comparing the peak position and height, bare DNA has persistence length L_p about 41.9 nm which is quantitatively in good agreement with the value of 43 nm that was calculated from $P(\theta)$ shown in Figure 2(b). By a similar comparison of MD data and the WLC calculation, dendrimer bound DNA is characterized by an effective persistence length L_p about 6.3 nm implying that the dendrimer bound DNA is 7 times more flexible than the bare DNA. However, the shape of $P(R)$ for dendrimer bound DNA is not well correlated with WLC results. This is due to the fact that the WLC model does not include the interaction of dendrimer. Moreover in MD simulations we have also solvent and counterion effects included which are not included in WLC model.

Force-extension curves calculated from WLC model are plotted in Figure 4(b) and compared with the interpolation formula of Marko-Siggia [8]. Note that the interpolation formula

for force-extension curve given by Marko-Siggia [8],

$$\frac{fL_p}{k_B T} = \epsilon + \frac{1}{4(1-\epsilon)^2} - \frac{1}{4} \quad (14)$$

is asymptotically valid for long polymers for small and large force limits. For stiff polymers, the force required to stretch is higher compared to flexible polymers. The Marko-Siggia [8] formula works well for large β over a wide range of forces. With the inclusion of the DNA intrinsic elasticity via stretch modulus γ_1 , Odijk [61] proposed the following interpolation formula,

$$\epsilon = \frac{R}{L_0} = \left[1 - \sqrt{\frac{k_B T}{4fL_p} + \frac{f}{\gamma_1}} \right] \quad (15)$$

which is valid for large β . Eqn. 15 is used to fit the force-extension curves obtained from MD simulations which is discussed in the next section.

B. A note from non-equilibrium stretching

From the stretching behavior, we can also estimate the elastic properties of DNA. For this, we have applied external force on one end of the DNA with the force applied on the O3' and O5' atoms of the two strands of the dsDNA respectively while keeping the other end (O5' of one strand and O3' of the other strand) fixed in order to mimic the single molecule stretching experiments in atomic force microscopy (AFM) or optical or magnetic tweezers. We have employed a time varying force ensemble where the force on DNA is increased with time and measured the extension as a function of the momentary pulling force. The total energy function of the system under the action of external force is given by

$$V(r^N) = V_o(r^N) + V_{\text{ext}}(t) \quad (16)$$

where $V_o(r^N)$ is the classical empirical potential describing the bonded and non-bonded interactions and $V_{\text{ext}}(t)$ is the potential under the action of external force used to stretch DNA which is given by

$$V_{\text{ext}}(t) = (R(0) - R(t))f(t) \quad (17)$$

In the above equation, $R(0) = R_0$ is the end-to-end vector distance at time 0, $R(t)$ is the end-to-end vector distance at time t and $f(t)$ is the time dependent force that acts along

end-to-end vector. We have used the force rates of 10^{-4} pN/fs and 10^{-5} pN/fs to stretch DNA of 38 base-pairs and 12 base-pairs, respectively since computational cost increases with the rate of forcing and system size. However, the obtained force-extension curve strongly depends on the rate of force applied.

Earlier we have studied the pulling rate dependence of the dsDNA stretching [41, 42]. Force-extension curves for 12 base-pair DNA at 10^{-5} pN/fs and 38 base-pair DNA at 10^{-4} pN/fs DNA are shown in Figure 5. With higher pulling rate the plateau in force-extension curve was observed at higher pulling force as expected. The end-to-end distance R is measured as the average end-to-end O3'-O5' atom distance of two strands when the force is zero. In the initial stage, as the force is increasing, the length of DNA increases linearly with the force [41, 42]. This is followed by a highly nonlinear regime called overstretching region where DNA gets stretched suddenly about 1.7 times its initial length with a very small increment in applied force. Our goal here is to understand how well the theoretical framework we have discussed so far helps in understanding the force-extension curves of DNA. We use $\gamma_1 = 955$ pN and $L_p = 43$ nm calculated from the equilibrium contour length and angle distributions to fit force-extension curves with Eqns. 14 and 15. Fitting is done with contour length L_0 as the fitting parameter. In Figure 5 we fit the force-extension curves to Eqns. 14, 15 and obtain contour length L_0 of 12.98 nm and 12.84, respectively for 38 base-pair DNA. Similarly fitting of Eqns. 14 and 15 gives 4.28 nm and 4.3 nm, respectively for 12 base-pair DNA. It is observed that the enthalpic elasticity included in Eqn. 15 by introducing f/γ_1 describes the simulation data very well for small forces since the contour length of DNA is much less than L_p . All of these formulas describe the force-extension curves quite well for small forces before the overstretching region. But they fail to explain the force-extension curve in overstretching region. The force response in the overstretching transition can be fitted by models that include the cooperative base-stretching transition [62], which however is not pursued in this paper. From this analysis, we get good agreement between Eqns.14, 15 and our MD results for small forces till the overstretching region. Hence we conclude that the non-equilibrium force-extension curves also support the observations made from equilibrium fluctuation analysis. Note that the equilibrium simulations are performed at Na^+ concentration of 275 mM for bare DNA and non-equilibrium simulations are performed at Na^+ concentration of 130 mM. Since

Eqns.14 and 15 ignore counterions and solvent effects which are properly treated in our MD simulations, there could be minor mismatch in the fits shown in Figure 5.

IV. CONCLUSION

We have calculated various elastic properties of a dsDNA from equilibrium fluctuation analysis and numerical solution to WLC model. The distribution of equilibrium contour length $P(L)$ and bending angle $P(\theta)$ are fit to Gaussian to calculate the stretch modulus γ_1 and persistence length L_p of DNA, respectively. The stretch modulus obtained from this equilibrium distribution is compared to the value obtained from the non-equilibrium stretching simulations. We also study how the elasticity of DNA is affected by protein binding with DNA, considering dendrimer as a model protein. We find that the DNA becomes 7-8 times flexible with respect to the fluctuations in the end-to-end distance when dendrimer binds to it. In the presence of dendrimer, the stretch modulus γ_1 of the DNA is 959 pN and the effective persistence length L_p is 6.3 nm compared to $\gamma_1 = 955$ pN and $L_p = 43$ nm for bare DNA. The calculated elastic parameters are in good agreement with the experimental calculations. Further by performing numerical calculations to solve WLC model, we calculate end-to-end distance distribution and force-extension curves of DNA for various lengths ranging from highly flexible to highly stiff polymers. We find good correlation with the equilibrium results. Force-extension curves for 12 base-pair DNA at 10^{-5} pN/fs and 38 base-pair DNA at 10^{-4} pN/fs were obtained. The non-equilibrium stretching simulations are compatible with the results obtained from equilibrium simulations. These results are helpful in understanding DNA elasticity at small length scales and the effect of protein interaction with DNA which is abundant in many cellular phenomena.

V. ACKNOWLEDGMENTS

We thank Yann von Hansen, Supurna Sinha and Rob Phillips for helpful discussions. SM acknowledges Erasmus Mundas fellowship from European Union and senior research fellowship from India. We acknowledge Department of Biotechnology (DBT), Government

of India for financial support.

- [1] Shore, D.; Langowski, J.; Baldwin, R. L. *Proc. Natl. Acad. Sci. USA*. **1981**, *78*, 4833–4837
- [2] Widom, J. *Q. Rev. Biophys.* **2001**, *34*, 269–324
- [3] Rippe, K.; Vonhippel, P. H.; Langowski, J. *Trends Biochem. Sci.* **1995**, *20*, 500–506
- [4] Smith, S. B.; Finzi, L.; Bustamante, C. *Science* **1992**, *258*, 1122–1126
- [5] Bustamante, C and Marko, J. F. and Siggia, E. D. and Smith, S, *Science* **1994**, *265*, 1599–1600
- [6] Smith, S. B.; Cui, Y. J.; Bustamante, C. *Science* **1996**, *271*, 795–799
- [7] Perkins, T. T.; Quake, S. R.; Smith, D. E.; Chu, S. *Science* **1994**, *264*, 822–826
- [8] Marko, J. F.; Siggia, E. D. *Macromolecules* **1995**, *28*, 8759–8770
- [9] Netz, R. R. and Joanny, J. F., *Macromolecules* **1999**, *32*, 9026–9040
- [10] Kunze, K. K. and Netz, R. R., *Phys. Rev. Lett.* **2000**, *85*, 4389–4392
- [11] Maiti, P. K.; Cagin, T.; Wang, G. F.; Goddard, W. A. *Macromolecules* **2004**, *37*, 6236–6254
- [12] Maiti, P. K.; Cagin, T.; Lin, S. T.; Goddard, W. A. *Macromolecules* **2005**, *38*, 979–991
- [13] Svenson, S.; Tomalia, D. A. *Adv. Drug Deliver. Rev.* **2005**, *57*, 2106–2129
- [14] Maiti, P. K.; Messina, R. *Macromolecules* **2008**, *41*, 5002–5006
- [15] Maiti, P. K.; Bagchi, B. *Nano Lett.* **2006**, *6*, 2478–2485
- [16] Nandy, B.; Maiti, P. K., *J. Phys. Chem. B* **2011**, *115*, 217–230
- [17] Ha, B. Y. and Thirumalai, D, *J. Chem. Phys.* **1995**, *103*, 9408–9412
- [18] Wilhelm, J.; Frey, E. *Phys. Rev. Lett.* **1996**, *77*, 2581–2584
- [19] Samuel, J.; Sinha, S. *Phys. Rev. E* **2002**, *66*, 050801
- [20] Dhar, A.; Chaudhuri, D. *Phys. Rev. Lett.* **2002**, *89*, 065502
- [21] Stepanow, S and Schutz, G. M., *Europhys. Lett.* **2002**, *60*, 546–551
- [22] Winkler, R. G., *J. Chem. Phys.* **2003**, *118*, 2919–2928
- [23] Valle, F and Favre, M and De Los Rios, P and Rosa, A and Dietler, G, *Phys. Rev. Lett.* **2005**, *95*, 158105
- [24] Ranjith, P.; Kumar, P. B. S.; Menon, G. I. *Phys. Rev. Lett.* **2005**, *94*, 138102
- [25] Hyeon, C. and Dima, R. I. and Thirumalai, D., *J. Chem. Phys.* **2006**, *125*, 194905
- [26] Seol, Y.; Li, J.; Nelson, P. C.; Perkins, T. T.; Betterton, M. D. *Biophys. J.* **2007**, *93*, 4360–4373
- [27] Mathew-Fenn, R. S.; Das, R.; Harbury, P. A. B. *Science* **2008**, *322*, 446–449

- [28] Yuan, C. and Chen, H. and Lou, X. W. and Archer, L. A., *Phys. Rev. Lett.* **2008**, *100*, 018102
- [29] Padinhateeri, R.; Menon, G. I. *Biophys. J.* **2013**, *104*, 463–471
- [30] Mazur, A. K., *Biophys. J.* **2006**, *91*, 4507–4518
- [31] Mazur, A. K. *Phys. Rev. Lett.* **2007**, *98*, 218102
- [32] Mazur, A. K. *J. Phys. Chem. B* **2009**, *113*, 2077–2089
- [33] Mazur, A. K. *Phys. Rev. E* **2009**, *80*, 010901
- [34] Chen, C.-Y. and Su, C.-J. and Peng, S.-F. and Chen, H.-L. and Sung, H.-W., *Soft Matter* **2011**, *7*, 61–63
- [35] Dootz, R. and Toma, A. C. and Pfohl, T., *Soft Matter* **2011**, *7*, 8343–8351
- [36] Boroudjerdi, H.; Naji, A.; Netz, R. R. *Eur. Phys. J. E.* **2011**, *34*
- [37] Bustamante, C.; Macosko, J. C.; Wuite, G. J. L. *Nature Rev. Mol. Cell Biol.* **2000**, *1*, 130–136
- [38] Gosse, C.; Croquette, V. *Biophys. J.* **2002**, *82*, 3314–3329
- [39] Lebrun, A.; Lavery, R. *Nucleic Acids Res.* **1996**, *24*, 2260–2267
- [40] Cluzel, P.; Lebrun, A.; Heller, C.; Lavery, R.; Viovy, J. L.; Chatenay, D.; Caron, F. *Science* **1996**, *271*, 792–794
- [41] Santosh, M. and Maiti, P. K., *J. Phys.: Condens. Matter* **2009**, *21*, 034113
- [42] Santosh, M. and Maiti, P. K., *Biophys. J.* **2011**, *101*, 1393–1402
- [43] Kratky, O.; Porod, G. *Recl. Trav. Chim. Pays-Bas-J. Roy. Neth. Chem. Soc.* **1949**, *68*, 1106–1122
- [44] Wiggins, P. A.; Van der Heijden, T.; Moreno-Herrero, F.; Spakowitz, A.; Phillips, R.; Widom, J.; Dekker, C.; Nelson, P. C. *Nature Nanotech.* **2006**, *1*, 137–141
- [45] Li, J.; Nelson, P. C.; Betterton, M. D. *Macromolecules* **2006**, *39*, 8816–8821
- [46] Bouchiat, C and Wang, M. D. and Allemand, J. F. and Strick, T and Block, S. M. and Croquette, V, *Biophys. J.* **1999**, *76*, 409–413
- [47] Livadaru, L and Netz, R. R. and Kreuzer, H. J., *Macromolecules* **2003**, *36*, 3732–3744
- [48] Storm, C and Nelson, P. C., *Phys. Rev. E* **2003**, *67*, 051906
- [49] Rosa, A.; Hoang, T.; Marenduzzo, D.; Maritan, A. *Biophys. Chem.* **2005**, *115*, 251–254
- [50] Toan, Ngo Minh and Thirumalai, D., *Macromolecules* **2010**, *43*, 4394–4400
- [51] Maiti, P. K.; Pascal, T. A.; Vaidehi, N.; Goddard, W. A. *Nucleic Acids Res.* **2004**, *32*, 6047–6056
- [52] Maiti, P. K.; Pascal, T. A.; Vaidehi, N.; Heo, J.; Goddard, W. A. *Biophys. J.* **2006**, *90*,

1463–1479

- [53] Duan, Y.; Wu, C.; Chowdhury, S.; Lee, M. C.; Xiong, G. M.; Zhang, W.; Yang, R.; Cieplak, P.; Luo, R.; Lee, T.; Caldwell, J.; Wang, J. M.; Kollman, P. *J. Comput. Chem.* **2003**, *24*, 1999–2012
- [54] Jorgensen, W. L.; Chandrasekhar, J.; Madura, J. D.; Impey, R. W.; Klein, M. L. *J. Chem. Phys.* **1983**, *79*, 926–935
- [55] Mayo, S. L.; Olafson, B. D.; Goddard, W. A. *J. Phys. Chem.* **1990**, *94*, 8897–8909
- [56] Darden, T.; York, D.; Pedersen, L. *J. Chem. Phys.* **1993**, *98*, 10089–10092
- [57] Ryckaert, J. P.; Ciccotti, G.; Berendsen, H. J. C. *J. Comput. Phys.* **1977**, *23*, 327–341
- [58] Lavery, R.; Skelnar, H. *J. Biomol. Struct. Dyn.* **1988**, *6*, 63–91
- [59] Becker, N. B.; Everaers, R. *Science* **2009**, *325*, 538
- [60] Noy, A.; Golestanian, R. *Phys. Rev. Lett.* **2012**, *109*, 228101
- [61] Odijk, T. *Macromolecules* **1995**, *28*, 7016–7018
- [62] Einert, T. R.; Staple, D. B.; Kreuzer, H.-J.; Netz, R. R. *Biophys. J.* **2010**, *99*, 578–587

Figures

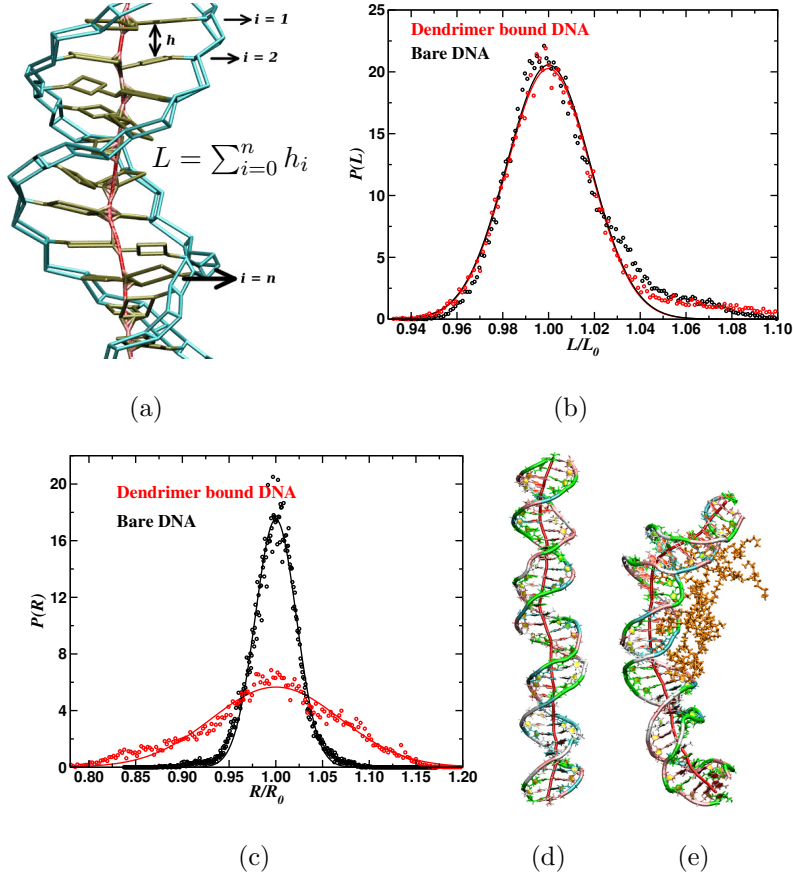


FIG. 1: *Equilibrium MD simulations: (a) Schematic showing the base-pair rise h and contour length L . (b) Contour length and (c) end-to-end distance distribution for 38 base-pair bare DNA and dendrimer bound DNA. Fitting $P(L)$ to a Gaussian gives a stretch modulus γ_1 of 955 pN for bare DNA and 959 pN for dendrimer bound DNA. Representative snapshots of 38 base-pair (d) bare DNA and (e) dendrimer bound DNA. We can see from plot of $P(R)$ and snapshots that the bare DNA is almost straight with less bending fluctuations, where as dendrimer bound DNA has large bending fluctuations. Color code: adenine - cyan, guanine - pink, thymine - white, cytosine - green, helix axis - red and dendrimer - orange.*

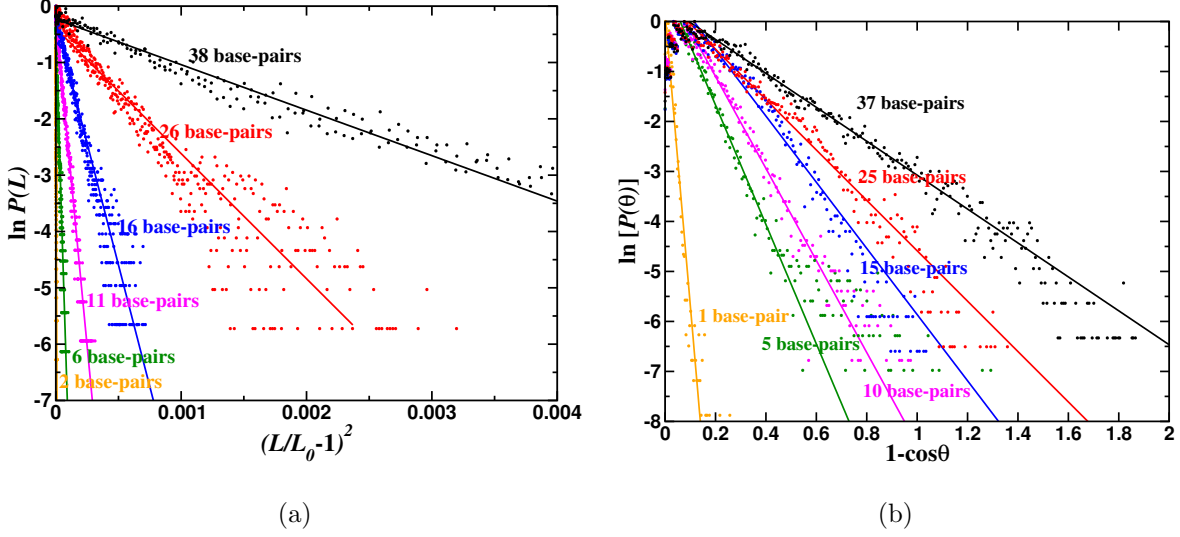


FIG. 2: Results for bare DNA: (a) Semi-log plot of contour length distribution $P(L)$ for various base-pair lengths. For all base-pair lengths, $P(L)$ is Gaussian and hence $\ln P(L)$ is linear in $(L/L_0 - 1)^2$. (b) Semi-log plot of bending angle distribution $P(\theta)$ for various base-pair lengths. The persistence length L_p calculated from the slope for 37 base-pair is 43 nm which is close to experimental findings.

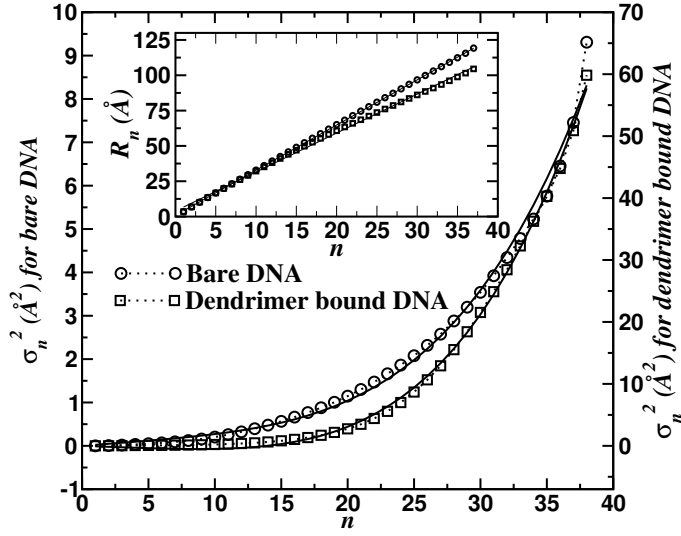


FIG. 3: Variance σ_n^2 in end-to-end distance as a function of the number of base-pairs n for bare DNA and dendrimer bound DNA. σ_n^2 is quartic in n . Inset shows average end-to-end distance R_n as function of n , $R_n \propto n$.

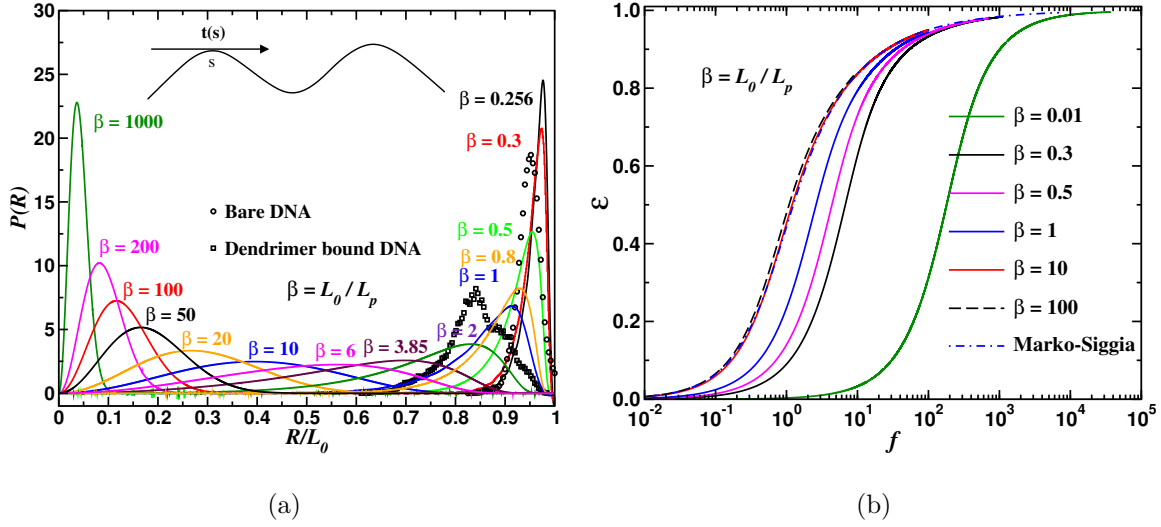


FIG. 4: Solution of WLC model using numerical calculations: (a) $P(R)$ for various β values, where $\beta = L_0/L_p$. Schematic of the WLC model is shown in the inset. We compare $P(R)$ of WLC model with $P(R)$ that is obtained from MD results for DNA and dendrimer bound DNA. $P(R)$ for dendrimer bound DNA is deviating from the WLC result since WLC model does not consider the dendrimer effect. (b) Force-extension curves for various β values. Analytical results of Marko-Siggia [8] is in good agreement with force-extension curve obtained by numerical simulation for large β .

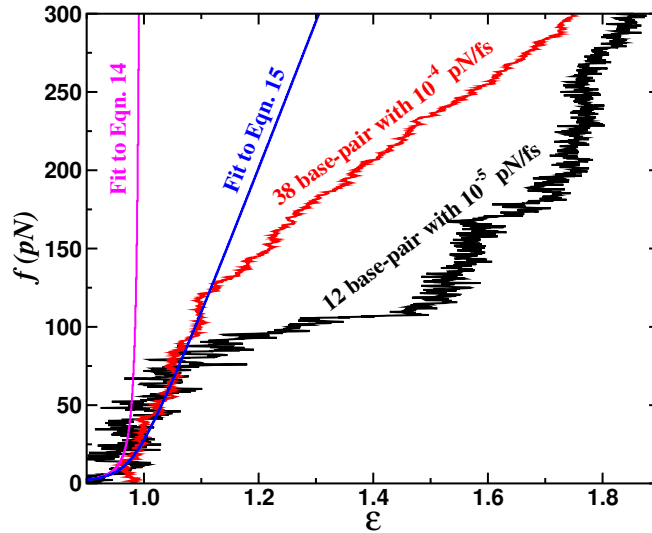


FIG. 5: *Non-equilibrium stretching of DNA using MD: Force-extension curve for 12 base-pair dsDNA at pulling rate of 10^{-5} pN/fs and 38 base-pair dsDNA at pulling rate of 10^{-4} pN/fs. We fit the force-extension curves obtained from MD simulations to Eqns. (14) and (15) with L_0 as fitting parameter and using $\gamma_1 = 955$ pN and $L_p = 43$ nm which are obtained from equilibrium $P(L)$ and $P(\theta)$, respectively.*